Drug Development and Industrial Pharmacy, 2010; 36(9): 1005–1015

informa
healthcare

ORIGINAL ARTICLE

Nondestructive rheological measurement of aqueous dispersions of solid lipid nanoparticles: effects of lipid types and concentrations on dispersion consistency

Nispa Seetapan[1], Piyawan Bejrapha[2], Wanwisa Srinuanchai[2], Satit Puttipipatkhachorn[3] and Uracha Ruktanonchai[2]

[1]National Metal and Materials Technology Center, National Science and Technology Development Agency, Pathumthani, Thailand, [2]National Nanotechnology Center, National Science and Technology Development Agency, Pathumthani, Thailand and [3]Department of Manufacturing Pharmacy, Faculty of Pharmacy, Mahidol University, Bangkok, Thailand

Abstract

Purpose: To investigate dispersion consistency of solid lipid nanoparticles as functions of lipid types and concentrations. *Methods:* Viscoelastic measurement at an application of low stress was employed to characterize the internal microstructure developed within the dispersions. Pure triglycerides with different length of fatty acid chains, trimyristin (C14), tripalmitin (C16), and tristearin (C18) were studied with respect to the partial triglyceride with C22 chain length (Compritol 888 ATO), and cetyl palmitate wax (C16). *Results and discussion:* Increasing fatty acid chain length of triglycerides induced more particle shape anisometry; therefore, elastic behavior of triglyceride dispersion increased in sequence of trimyristin < tripalmitin < tristearin. Because of an imperfect crystalline structure, Compritol 888 ATO particles yielded the dispersion with a less elastic behavior. Despite having an equal fatty acid chain length (C16), cetyl palmitate wax provided the dispersion with lower network strength than tripalmitin as a result of the lower ordered crystal packing of fatty acid chains in the wax particle. Increasing lipid concentration improved the dispersion consistency owing to the more pronounced interaction between lipid particles. Data obtained from particle size analysis did not help explain the resulting microstructures in relation to the types and concentrations of lipid. *Conclusions:* A nondestructive rheological experiment is a powerful tool in revealing the microscopic structures of SLNs, which provides the information on viscous and elastic behaviors, corresponding to the internal structure of the dispersions. Consequently, viscoelastic data might assist pharmaceutical industry in selecting type of lipid appropriate for developing SLN formulations with the desired consistency.

Key words: *Lipid structure; rheology; solid lipid nanoparticles; triglyceride; viscoelastic*

Introduction

In recent years, much attention has been focused on lipid-based pharmaceutical formulations to improve the bioavailability of water-insoluble compounds. In fact, the most popular approach is the incorporation of the active lipophilic component into inert lipid vehicles such as oils, surfactant dispersions, emulsions, and liposomes[1,2]. Solid lipid nanoparticles (SLNs), a colloidal system consisting of lipid and emulsifying agents that are solid at room temperature, have recently gained much interest as an alternative drug carrier because of their submicron size, potential for industrial scale production, and their composition of physiological lipids. SLNs were first developed by Müller and Lucks[3] and have been used as a colloidal drug carrier not only for dermal delivery[4] but also for intravenous[5], ocular[6], and oral administrations[7].

The consistency of SLN delivery systems can be varied from liquid to semisolid properties, which potentially influences cosmetic and pharmaceutical applications[8–11]. For dermal formulations, such as creams, ointments,

Address for correspondence: Dr. Nispa Seetapan, National Metal and Materials Technology Center, National Science and Technology Development Agency, 114 Thailand Science Park, Paholyothin Road, Pathumthani 12120, Thailand. Tel: +66 25646500, Fax: +66 25646445. E-mail: nispam@mtec.or.th

(Received 10 Aug 2009; accepted 30 Dec 2009)

ISSN 0363-9045 print/ISSN 1520-5762 online © Informa UK, Ltd.
DOI: 10.3109/03639040903586273

pastes, and gels, it is necessary that they should adhere to skin. A relatively high viscosity and a thixotropic flow behavior are therefore required. On the other hand, parenteral administration generally prefers low-viscosity formulations for easy injection[12]. From this point of view, rheological characterizations, based on steady shear flow (rotational) and oscillation (dynamic) experiments, are particularly important for the development of SLN formulations for such administrations. Several pharmaceutical materials are semisolids whose properties combine characteristics of both liquid and solid. Viscoelastic behavior is, consequently, one of the important rheological properties in revealing the internal microstructure of viscoelastic materials at rest. Because viscoelastic measurements are nondestructive, they can provide information on the structure and elasticity, and the storage stability of a material. Furthermore, the influence of released drug from a vehicle can be investigated by these measurements[13]. Several parameters, such as type and concentration of lipid matrix, particle size, and shape of lipid, are critical factors that affect viscoelastic properties of the prepared SLNs.

Oscillatory measurement is typically used to measure viscoelastic properties of materials[14–16]. To obtain information on the internal microstructure, material is basically exposed to a sinusoidal oscillatory stress (or strain) whose amplitude is smaller than the critical value, the resulting strain (or stress) and phase lag (δ) between the input stress and the output strain are measured. This type of deformation can provide information on elastic energy storage and viscous energy dissipation, quantitatively represented as storage modulus (G') and loss modulus (G''), respectively. G' is proportional to the extent of the elastic component providing from crosslinking, entanglement, or aggregation in the system. G'' is rational to the extent of the viscous component (from the liquid-like portion) of the system. The strength of materials is quantified by the magnitude of tan δ, which is the ratio of G''/G'.

Several solid lipids have been employed to prepare drug-loaded SLNs[4,11,17–20]; however, most of the works have been focused only on crystallization behaviors, release profiles, and skin penetration studies of drugs from the SLN vehicles. On the contrary, the information on rheological behaviors of SLNs with and/or without loaded drugs is rather limited. Basically, the quantity of loaded drug in the lipid vehicle is fairly low; hence, the lipid matrix typically determines rheological properties of the final SLNs. Dependence of dispersion consistency on particle size of cetyl palmitate wax has been reported by Lippacher et al.[21] By performing nondestructive oscillatory experiments, they demonstrated that nanoparticle dispersion provided a semisolid consistency suitable for topical application; while microparticle dispersion showed viscous behavior.

Viscoelastic behaviors of aqueous dispersions of SLNs and nanoparticle lipid carriers (NLCs) were soon after characterized by Souto et al.[22] Different types of liquid oil were found to have a strong influence on viscoelastic properties of the NLC formulations. Lippacher et al.[23] studied the effect of lipid concentration on dispersion consistency of concentrated SLN formulations prepared from cetyl palmitate wax and found the increase in storage modulus, indicating a more elastic gel as increasing lipid concentration.

Different flow behaviors of SLN dispersions were characterized as functions of type and concentration of triglycerides, suspension stabilizers, and added electrolytes[12]. However, in the study of flow properties, a continuous variation of shear rate (or shear stress) was applied to the material, and the apparent viscosity and shear stress (or shear rate) were measured by the rheometer. The steady shear flow was a destructive measurement that could not provide the information on an internal microstructure of the viscoelastic material.

Storage stability of nanoparticles has been detected through viscoelastic measurement. Junyaprasert et al.[24] demonstrated that an increase in dispersion consistency during storage time of 6 months at 20°C of Q_{10}-loaded NLCs incorporated into xanthan gum hydrogels was observed from monitoring the increase of storage modulus, resulting from the occurrence of a spatial arrangement of lipid molecules. Seetapan et al.[25] found that upon storage γ-oryzanol-loaded SLNs over 2 months at 4°C, 25°C, and 40°C, all formulations showed the enhanced consistency because of the gel formation with the increase in storage modulus. Especially at the storage temperature of 40°C, the pronounced instability was also detected from scanning electron micrographs as the formation of rod-like network structure possibly from the coalescence of spherical nanoparticles.

Although the dispersion consistency of SLN formulations has been reported as previously described through viscoelastic characterization, those investigations did not reveal effect of the use of different lipid types on dispersion consistency under the same composition. Furthermore, several studies on viscoelasticity of SLNs were generally performed on concentrated lipid dispersions, which typically showed semisolid property. Therefore, the variations in dispersion consistency of SLN formulations acquired from the use of different types of lipid at both low and high lipid concentrations were investigated in this study using nondisruptive low-stress oscillatory experiments to preserve the molecular structure of the prepared systems. Types of solid lipid were selected from the frequently employed lipids in several literatures dealing with SLN formulations. A series of triglycerides with different fatty acid chain lengths between 14 and 18 of saturated carbons (Dynasan 114–118) was chosen to study the effect of fatty acid chain

length of the triglycerides. Triglycerides are esters of fatty acids with glycerols. Dynasan 114 contains a portion of 4% di- and 95% triglycerides of myristic acid (C14). Dynasan 116 is a combination of 3% di- and 96% triglycerides of palmitic acid (C16). Dynasan 118 is a mixture of 2% di- and 97% triglycerides of stearic acid (C18). The partial triglyceride, Compritol 888 ATO, was also employed for a comparison. Compritol 888 ATO is a blend of 12–18% mono-, 52–54% di-, and 28–32% triglycerides of behenic acid (C22), a major fraction of fatty acid (>85%); however, other fatty acids with C16–C20 is also present[26]. A solid cetyl palmitate wax ($C_{16}H_{33}$–O–CO–$C_{15}H_{31}$), an ester of cetyl alcohol (C16) with palmitic acid (C16), was studied comparatively to the triglyceride containing the same length of fatty acid (Dynasan 116). The comparison between viscoelastic behaviors and dispersion consistency of different SLN formulations was discussed. Knowledge about viscoelastic behaviors of SLNs prepared from the investigated solid lipids can help to understand dispersion consistency of the nanoparticle systems prepared from different types and concentrations of lipid.

Materials and methods

Materials

The following materials were used as received without further purification procedures. Cetyl palmitate was obtained from P. Intertrade, Ltd. (Gastafosse, Spain). Triglycerides, namely, Dynasan 114 (trimyristin), Dynasan 116 (tripalmitin), and Dynasan 118 (tristearin), were received from Sasol (Witten, Germany). Compritol 888 ATO (glycerol behenate) was obtained from P. Intertrade, Ltd. The surfactant Tegocare 450 (polyglyceryl glucose methyl distearate) was from ZI-Techasia Solutions Ltd. (Goldschmidt, Germany). Water was obtained from a Milli-Q Plus purification system (Millipore, Schwalbach, Germany), and all other reagents employed were commercially available and of analytical grade.

Solid lipid nanoparticles preparation

The preparation of aqueous SLN dispersions was carried out according to Müller and Lucks[3]. Aqueous dispersions of SLNs, composed of lipid phase and 2.5% by weight of surfactant (Tegocare 450), were produced using the hot homogenization technique. The concentrations of lipid employed were 5% and 20% (w/w). The lipids were heated above their melting points and dispersed under high-speed stirring (6500 rpm) for 5 minutes using an Ultra-Turrax T25 (IKAWerke, Staufen, Germany) in the hot aqueous surfactant solution of identical temperature. This pre-emulsion was subsequently subjected to a high-pressure homogenizer (EmulsiFlex-C3, Avestin, Ontario, Canada) for three cycles at a pressure of 1500 bar. After homogenization, the produced dispersions were cooled down and solidified to obtain the aqueous SLN dispersions.

Rheological measurements

Viscoelastic behaviors were obtained using a controlled-stress Gemini HR^{nano} rheometer (Malvern Instruments Ltd., Worcestershire, UK), which was able to operate at the nano-torque levels enabling to probe weak or sensitive structure. The instrument was equipped with 55- or 20-mm diameter stainless steel plate fixture depending on the sample viscosity, and 1 mm gap size. To prevent the slip of the sample during measurement, sand papers were attached to the upper and lower plates of the fixture. A solvent-trap system was attached to the instrument to prevent water evaporation during measurement. The operating temperature was 25°C, controlled by a peltier plate. Linear viscoelastic (LVE) region was determined by performing oscillatory stress sweep experiment from 0.01–100 Pa at a fixed frequency of 1 Hz. Oscillatory frequency sweep experiment was subsequently carried out at a fixed stress within the determined LVE range.

Determination of hydrodynamic diameter and zeta potential

The hydrodynamic diameter, polydispersity index (PDI), and zeta potential of the nanoparticles were determined by photon correlation spectroscopy (PCS) and electrophoretic mobility titration (NanoZS4700 nanoseries, Malvern Instruments). For size measurement, all formulations were diluted with 1 mL of 0.22-μm filtered deionized water to eliminate the effect of viscosity caused by the ingredients. The zeta potential measurements were performed in distilled water, which was adjusted to a conductivity of 50 μS/cm with 0.90% (w/v) sodium chloride solution. The hydrodynamic diameter, PDI, and zeta potential were obtained as the average of three measurements at 25°C. The refractive indexes of SLNs and water were set at 1.46 and 1.33, respectively. The reported values are the average of at least three measurements.

Atomic force microscopy

The morphology of SLNs was analyzed by using an atomic force microscope (AFM, SPA400, Seiko, Chiba, Japan). Appropriate amounts of SLNs were diluted with distilled water and were dropped to freshly cleaved mica. After that the samples were placed in an atmosphere

until completely dry. Subsequently, the samples were imaged by scanning 5 × 5 μm area in tapping mode using an NSG01 cantilever with 115–190 kHz resonance frequencies and a constant force, in the range 2.5–10 N/m. All images were recorded in air at room temperature and a scan speed of 1 Hz, the phase image and topology image were used to determine the morphology of SLNs.

Results and discussion

SLNs with 5% (w/w) lipid dispersion

The preparation of SLNs from various types of solid lipid yielded the dispersions with dissimilar consistency. The dispersions of 5% (w/w) lipid prepared from cetyl palmitate, Dynasan 114, and Compritol 888 ATO appeared as liquid when visualized macroscopically, whereas Dynasan 116 and Dynasan 118 showed creamy (or semisolid) appearance. These consistency variations were according to the different internal microstructures developed within the dispersions and could be revealed by their viscoelastic behaviors through oscillatory measurements. Because the investigated systems are dispersions of electrostatically stabilized solid lipid particles in an aqueous phase, the presence of charges on the particle surface generates expanded double layers around the particles. The interference between double layers generates a repulsive force between particles. The extent of this interaction reflects the degree of elastic behavior in the dispersion. Therefore, the developed internal microstructure in electrostatically stabilized dispersions is dominated by the interaction between dispersed particles via double layer repulsion[27]. To determine viscoelastic behaviors, LVE region, where storage (G') and loss (G'') moduli are independent of the applied stress, was firstly determined through an oscillatory stress sweep at a fixed frequency of 1 Hz. Figure 1a and b showed the values of G' and tan δ, respectively, obtained from oscillatory stress sweep experiments of 5% (w/w) lipid. Figure 1a revealed that the width of LVE range was varied for each sample as observed from the deviation of the value of G' from linearity with increasing applied stress. To gain more insight into the stress-induced structural breakdown, the stress-dependent tan δ was plotted in Figure 1b. Tan δ is the ratio of G''/G'. If the value of tan δ is larger than 1 ($G'' > G'$), the system behaves more like viscous liquid, whereas if the value of tan δ is smaller than 1 ($G'' < G'$), the system shows more elastic (gel or network) behavior. The result indicated that Dynasan 114 dispersions showed a viscous liquid response because tan δ was larger than 1 for the entire stress ranges. On the other hand, other samples showed a gel-like response (tan $\delta < 1$) at low stress and turned to a liquid-like behavior (tan $\delta > 1$) as the applied stress increased. Therefore, one could predict that there was no network structure formation in 5% (w/w) Dynasan 114 dispersion, meaning that the interaction (or the contact) between particles was small. The value of tan δ can be used to describe strength of the internal network structure formed by particle–particle interactions in the investigated dispersions. The result of tan δ suggested that the network strength increased in an order of dispersion prepared from cetyl palmitate < Compritol 888 ATO < Dynasan 116 < Dynasan 118; moreover, the network capacity to withstand the maximum stress was in the same sequence.

For the systems containing network structure, the maximum stress up to which G' remains constant is called the critical stress (σ_c), which indicates a transition from linear to nonlinear regimes. The critical stress can be taken as the dynamic yield stress. This means that below the critical stress the system behaves like an elastic gel. At the external applied stress beyond σ_c, the internal network structure starts to break down and subsequently material flows like a liquid. The result shows that the LVE range and the critical stress increased orderly in dispersions prepared from cetyl palmitate < Compritol 888 ATO < Dynasan 116 < Dynasan 118. Wide LVE region and large σ_c indicated the system's ability to resist external stress to a greater extent.

Oscillatory frequency sweep measurements of SLN dispersions at 5% (w/w) lipid were investigated within the determined LVE region (Figure 1c and d). The obtained results provided the information on an internal network structure, which was the characteristic behavior of each system. The results indicated that Dynasan 116 and Dynasan 118 dispersions showed elastic behavior as G' remained frequency-independent over two decades of the investigated frequencies (Figure 1c) and the values of tan δ were smaller than 1 at all frequencies studied (Figure 1d). These behaviors corresponded to a viscoelastic solid with infinite relaxation time. The equilibrium storage modulus (G'_e), the plateau G' independent of the applied frequency, was observed in dispersions of Dynasan 116 and Dynasan 118 where the values of G'_e were correspondingly about 200 and 5000 Pa. G'_e is directly related to the density of network structure meaning that the network structure of 5% Dynasan 118 was stronger than that of 5% Dynasan 116.

Cetyl palmitate and Compritol 888 ATO dispersions showed a liquid to gel transition at a cross-over frequency, f_c, where tan δ is equal to 1 ($G' = G''$)[28] as shown in Figure 1d. The point at f_c is regarded to the gel point. At frequencies lower than f_c, both systems flowed as liquid (tan $\delta > 1$), whereas the systems possessed elastic property (tan $\delta < 1$) at frequencies beyond f_c. The f_c can be used as a rough estimation of the characteristic network relaxation time ($\tau = 1/2\pi f_c$), which is useful in

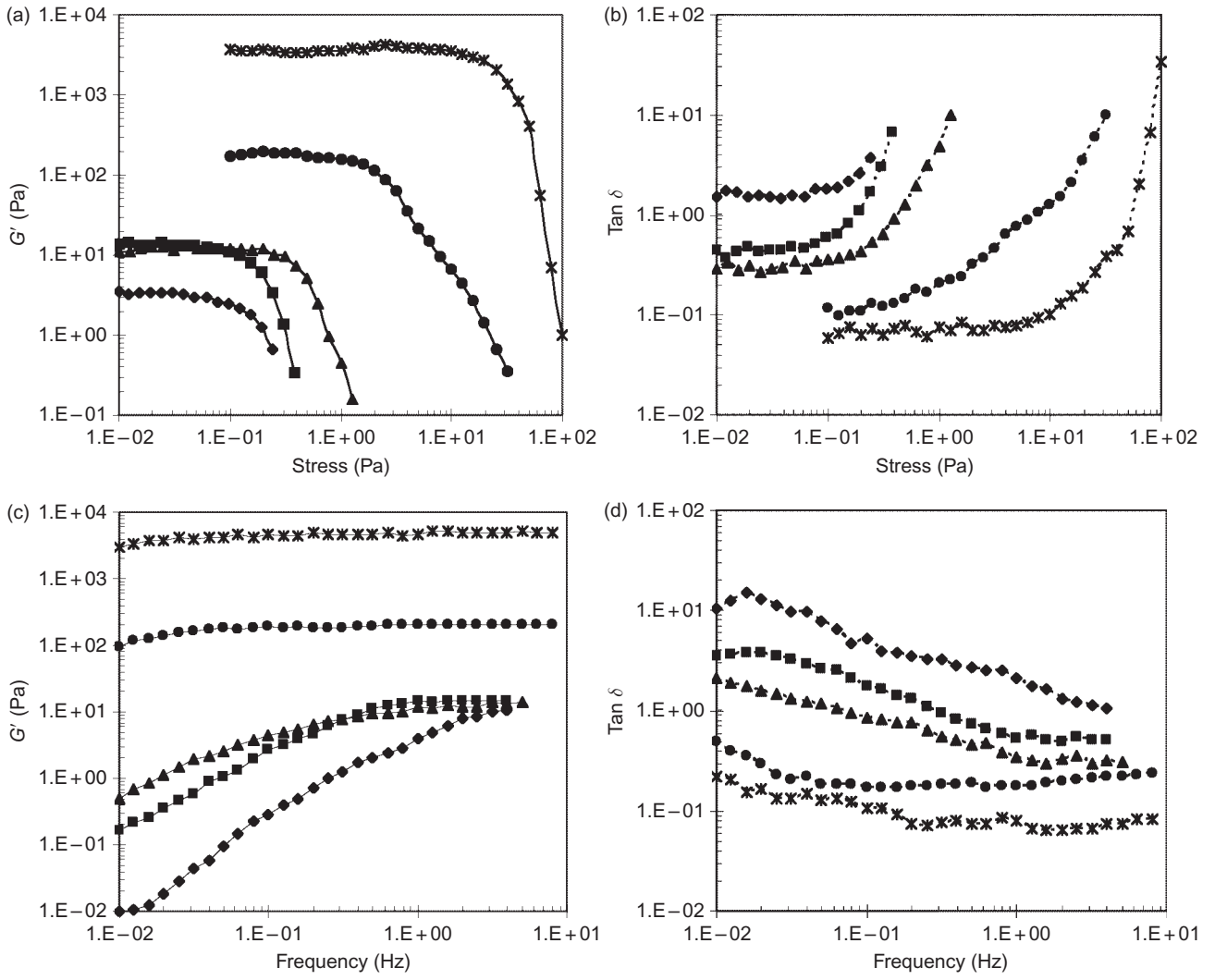

Figure 1. (a) Storage modulus (G') and (b) tan δ as a function of stress, and (c) storage modulus and (d) tan δ as a function of frequency of SLN dispersions at 5% (w/w) lipid: cetyl palmitate (■), Dynasan 114 (◆), Dynasan 116 (●), Dynasan 118 (*), Compritol 888 ATO (▲).

describing the tendency of flow behaviors of materials[27]. Hence, for 5% (w/w) dispersions, the values of relaxation time of cetyl palmitate and Compritol 888 ATO were about 0.5 and 2.7 seconds calculated from $f_c \sim$ 0.3 and 0.06 Hz, respectively. This means that if the relaxation time is smaller than the reciprocal of the rate of deformation (i.e., frequency), the system has sufficient time to relax to its equilibrium state, so that a fluid-like behavior is observed. In contrast, if the deformation time scale is much smaller than the relaxation time (i.e., at high frequencies of deformation), the system shows a gel-like response. At high frequencies where both systems transformed into gel, although G'_e of 5% (w/w) cetyl palmitate and 5% (w/w) Compritol 888 ATO dispersions were nearly equivalent (15 and 13 Pa, respectively), the dispersion of Compritol 888 ATO yielded a more elastic network as observed from the lower value of tan δ shown in Figure 1d.

In the dispersion of 5% (w/w) Dynasan 114, on the other hand, the plateau of G' was not observed and G' rapidly decreased with decreasing frequency. The value of tan δ was larger than 1 and it decreased with increasing frequency. The system therefore behaved as a typical viscoelastic liquid with a short relaxation time[29]. Table 1 summarizes the parameters taken from viscoelastic studies of 5% (w/w) lipid dispersions. Consistent to the obtained consistency, the semisolid behaviors of Dynasan 116 and 118 dispersions were due to their large values of the frequency-independent G'_e expanding over a wide range of frequency. Network structure of the dispersion from Dynasan 116 was softer than that from Dynasan 118 because of the smaller values of σ_c and G'_e. The decrease in dispersion consistency was accompanied by small values of τ, σ_c, and G'_e. Therefore, the presence of viscoelastic network is responsible for the increased consistency of the formulation.

Table 1. Critical stress (σ_c), equilibrium storage modulus (G'_e), the characteristic network relaxation time[a] (τ), and the appearance of SLN dispersions at 5% (w/w) lipid

Lipid at 5% (w/w) dispersion	σ_c (Pa)	G'_e (Pa)	τ (seconds)	Appearance
Cetyl palmitate	0.05	15	0.5	Liquid
Dynasan 114	N/A	N/A	0.04	Liquid
Dynasan 116	1	200	N/A	Cream
Dynasan 118	10	5000	N/A	Cream
Compritol 888 ATO	0.2	13	2.7	Liquid

[a] $\tau = 1/(2\pi f_c)$, where f_c is a frequency at which tan δ is equal to 1.

The investigated viscoelastic behaviors were explained in view of lipid types as follows. Among pure triglyceride dispersions at 5% (w/w), Dynasan 114 showed fluid-like response, whereas Dynasan 116 and 118 yielded elastic or gel-like behavior. The magnitude of storage modulus increased in the sequence of Dynasan 114 < Dynasan 116 < Dynasan 118. Because the elastic response in dispersion or emulsion is endowed by the interparticle interaction, various factors such as volume fraction, size, shape, and size distributions of the dispersed phase control the magnitude of such interaction. Typically, small particles have large surface area; therefore, the number of contacts between particles increases. As a consequence, interparticle interactions are marked, which lead to a strong elastic response. By increasing the particle size dispersity, the viscosity can be reduced[27]. In this study, the calculated volume fraction occupied by solid lipids in all 5% (w/w) dispersions was the same (about 0.05). The volume fraction was determined from known weight and density of all ingredients in the systems. Particle size analysis of the dispersions by means of PCS yielded the mean hydrodynamic diameter and the PDI as shown in Table 2. The particle diameter of 5% (w/w) lipid was in a nano-scale, approximately between 160 and 260 nm. The PDI of these SLN dispersions ranged from 0.15 to 0.38, suggesting that all formulations demonstrated a relatively narrow size distribution. The surface charge measurement of all dispersions revealed the dispersion stability with high value of zeta potential, approximately ranging from –38 to –57 mV (Table 2). The minus sign of zeta potential value represents the negative charges on particle surface. It is believed that when the absolute value of the zeta potential is higher than 30 mV for colloidal formulation, the particles are likely to be electrochemically stable under the investigated condition[9,19,30].

Table 2. Mean particle diameter, polydispersity index (PDI), and zeta potential of SLN dispersions at 5% (w/w) lipid.

Lipid system	Hydrodynamic diameter (nm)	PDI	Zeta potential (mV)
Cetyl palmitate	171 ± 0	0.15 ± 0.01	−53.6 ± 1.6
Dynasan 114	162 ± 3	0.13 ± 0.01	−57.7 ± 2.4
Dynasan 116	187 ± 2	0.23 ± 0.02	−54.9 ± 1.2
Dynasan 118	261 ± 29	0.38 ± 0.02	−38.2 ± 4.9
Compritol 888 ATO	152 ± 1	0.16 ± 0.02	−51.8 ± 1.2

Although the determined particle size and size dispersity revealed little difference between different lipid matrices, distinct rheological behaviors were obtained relevant to the obtained consistencies. It is interesting to note that PCS characterized particle size by assuming spherical shape. However, from AFM analysis of our selected 5% (w/w) Dynasan 114 formulation, a plate-like structure was observed as shown in Figure 2. PCS therefore cannot represent a real dimension of platelet-like particles[31] like the case of pure triglycerides. Illing and Unruh[12] investigated the flow behavior of Dynasan 114, Dynasan 116, and Dynasan 118 dispersions at the triglyceride content up to 20% (w/w) with a combination of phospholipids and sodium glycocholate or cetylpyridinium chloride as a dispersion stabilizer. They found that at the same lipid concentration, viscosity of dispersion matrix increased as the length of fatty acid increased. Triglycerides showed platelet-shaped nanocrystals in dispersions by an observation using electron micrographs. Therefore, increasing length of fatty acid chains led to more anisometric triglyceride crystals and higher dispersion viscosities. Like the inorganic platelets of bentonite or monoglyceride, the network structure of these nanocrystal dispersions were visualized as plates stacked in a 'house of cards'-type arrangement[32–34]. With regard to the particle shape, dispersion viscosity increases as the particle shape deviates from sphere because of the increasing number of contact between dispersed particles[35,36]. As a result, the increases of network strength and the critical stress of dispersion were likely corresponding to the increasing contact between anisometric particles, attributed by the increased length of fatty acid chains.

Dispersion of 5% (w/w) Compritol 888 ATO yielded the lower network strength and the smaller critical stress in comparison with Dynasan 116 and Dynasan 118 dispersions, although it contains more than 85% by weight of longer chains of fatty acid (C22). This might be resulted from its composition containing a variety of mixture of mono-, di-, and triglycerides, which could restrict the formation of highly ordered crystal packing of long-chain fatty acid arrangement providing lipid particle a lot of lattice defects[37]. The presence of lattice defects in the structure of lipid particle imparts softer particle–particle interaction in contrast to the interaction between dense particles. Unlike pure triglycerides, atomic force micrograph of Compritol 888 ATO dispersion revealed spherical particles (Figure 3). Similar observation was previously reported in literatures[25,38]. Besides the spherical shape that provides less particle

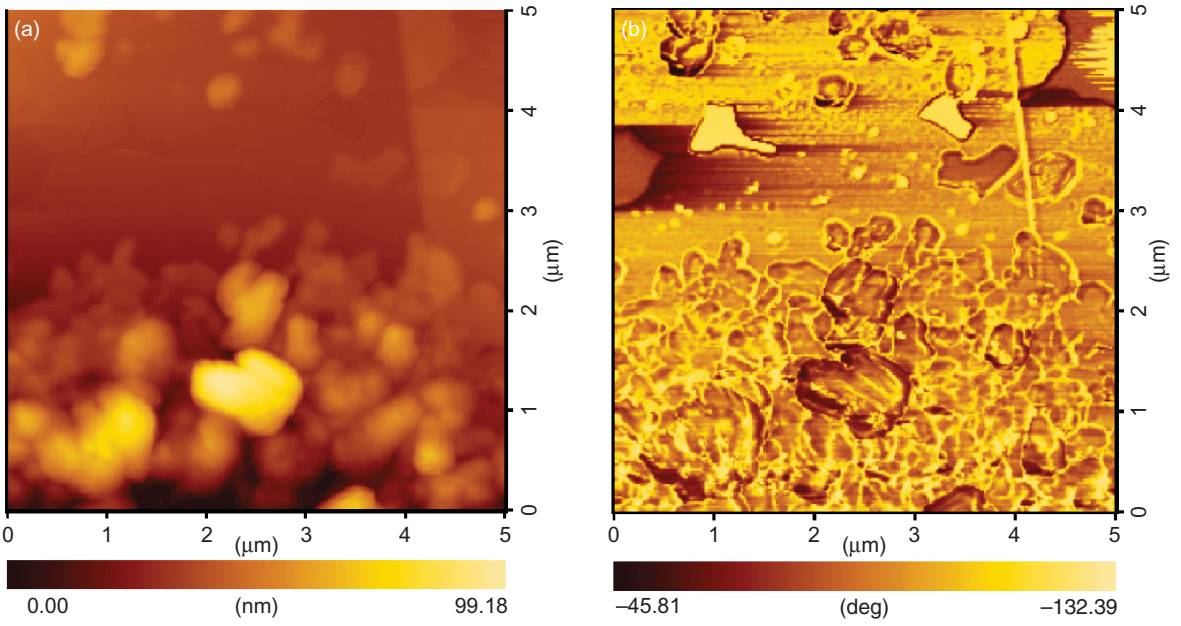

Figure 2. Particle morphology of 5% (w/w) Dynasan 114 dispersion observed by AFM. (a) Topographic and (b) phase images. All images were scanned at a 5 × 5 µm area.

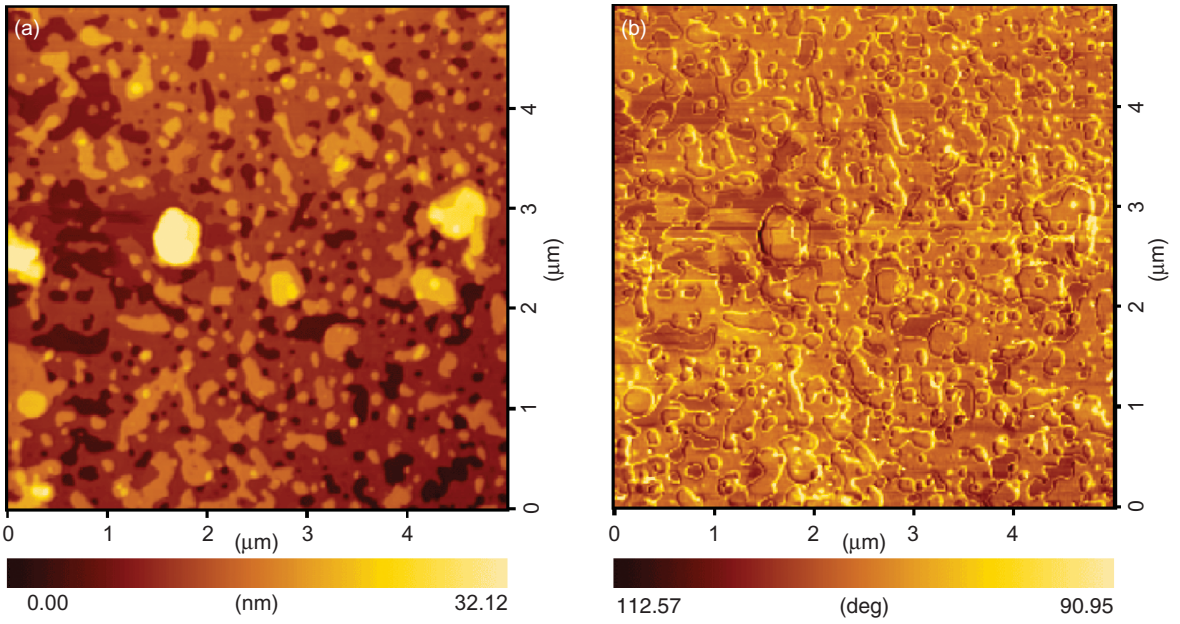

Figure 3. Particle morphology of 5% (w/w) Compritol 888 ATO dispersion observed by AFM. (a) Topographic and (b) phase images. All images were scanned at a 5 × 5 µm area.

contact, the presence of disordered lattice in particles of Compritol 888 ATO yielded dispersion less consistency than plate-like structure with highly ordered crystal packing of Dynasan 116 and Dynasan 118 particles.

Despite having an equal fatty acid chain length of C16 of cetyl palmitate and Dynasan 116, a dispersion of 5% cetyl palmitate wax revealed a much weaker and more sensitive structure than 5% Dynasan 116 dispersion because of the lower values of critical stress and equilibrium storage modulus. Cetyl palmitate nanoparticles were found to crystallize in a plate-like structure as confirmed by atomic force microscopy[20]. The structure of cetyl palmitate is composed of only one molecule of C16 fatty acid chain length connected with a cetyl alcohol (C16)

through ester linkage. On the other hand, the structure of Dynasan 116 triglyceride comprises three molecules of long-chain fatty acid (C16) consecutively connected to all carbon atoms of a glycerol. Therefore, the particle of Dynasan 116 might have a denser packing of fatty acid chains over the particle of cetyl palmitate wax. This resulted in a stronger interaction force between particles and a higher semisolid consistency in Dynasan 116 dispersion.

SLN with 20% (w/w) lipid dispersion

To investigate the effect of lipid concentration, nanoparticle dispersions at 20% (w/w) lipid were prepared. The dispersion consistency varied from liquid to solid upon types of lipid. The preparation of 20% (w/w) lipid dispersions from Dynasan 116 and 118 resulted in solid products that were capable of completely holding up the aqueous phase employed in the preparation step. The obtained solid consistency was probably due to the formation of high degree of hydrophobic association of long hydrocarbon fatty acid chains in both systems inducing the dispersion aggregation. Cetyl palmitate and Dynasan 114 yielded the dispersions with the ability to flow when the containers were tilted. The dispersion of 20% (w/w) Compritol 888 ATO was soft waxy-like to the touch that resisted flow under gravity.

As a result, viscoelastic measurements were performed only on cetyl palmitate, Dynasan 114, and Compritol 888 ATO dispersions. Figure 4a shows the effect of applied stress on storage modulus. Within the investigated stress range, the critical stress was not noticed in 20% (w/w) Compritol 888 ATO dispersion and the dispersion possessed very high values of G'. In addition, the dispersion demonstrated elastic behavior ($\tan\delta < 1$) for all the applied stresses (Figure 4b). In contrast, G' of

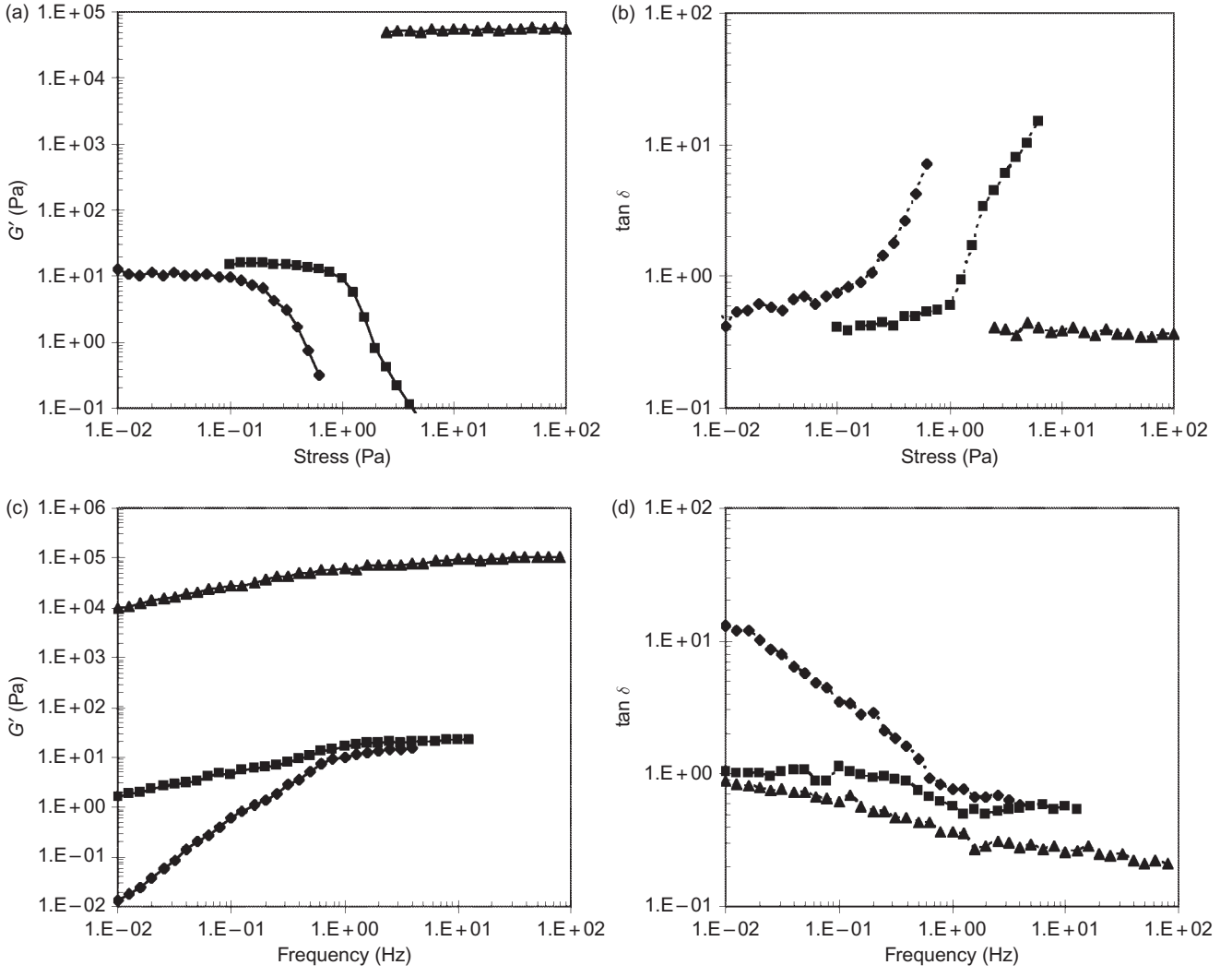

Figure 4. (a) Storage modulus (G') and (b) tan δ as a function of stress, and (c) storage modulus and (d) tan δ as a function of frequency of SLN dispersions at 20% (w/w) lipid:cetyl palmitate (■), Dynasan 114 (◆), Compritol 888 ATO (▲).

20% (w/w) cetyl palmitate and Dynasan 114 dispersions were about three or four decades lower. The critical stress was observed at about 0.5 and 0.08 Pa for cetyl palmitate and Dynasan 114 systems, respectively.

From oscillatory frequency sweep experiments (Figure 4c and d), the behaviors of 20% (w/w) cetyl palmitate and Compritol 888 ATO systems were similar in that at high frequencies; the plateau G' was observed. A large increase in the value of G' of Compritol 888 ATO over cetyl palmitate at 20% (w/w) was observed in contrast to the behaviors at 5% (w/w) where the magnitudes of G' for both systems were not significantly different. This might be from the higher possibility of many long chains of fatty acid in Compritol 888 ATO to self-associate leading to a huge increase in G' of 20% (w/w) dispersion. Because the crystalline particle of Compritol 888 ATO was less ordered as compared with the pure triglyceride particles, one could expect the semisolid consistency with the softer and more sensitive network structure in Compritol 888 ATO dispersion. Thereby, a decrease in G' at low-frequency ranges was observed and the value of tan δ started to increase as the frequency decreased. The cross-over frequency was approximately 0.01 Hz, corresponding to $\tau \sim 16$ seconds. Likewise, cetyl palmitate dispersion possessed a weak network structure because of the decrease of G' with decreasing frequency. The gel point expanded over a wide range of frequency (0.01–0.25 Hz). Therefore, the characteristic relaxation time was about 0.63 seconds, determined from the largest f_c (0.25 Hz). With the obtained liquid consistency, however, 20% (w/w) Dynasan 114 dispersion showed a cross-over from fluid to gel behavior with a weak network structure (from the value of tan δ in Figure 4d) and the characteristic network relaxation time of about 0.25 seconds.

Table 3 shows data characterized from viscoelastic studies of 20% (w/w) lipid dispersions. Comparative to 5% (w/w) lipid (Table 1), the magnitudes of critical stress, equilibrium storage modulus, and network relaxation time increased with lipid concentration because of the more elastic interaction force from the increased particle–particle contact.

Particle size and charge of 20% (w/w) dispersions were characterized and shown in Table 4. The determined absolute values of zeta potential of all particle dispersions were above 30 mV, indicating dispersion stability. The values of particle size of cetyl palmitate, Dynasan 114, and Dynasan 116 in 20% (w/w) dispersions were close to those in 5% dispersions despite the considerable difference in system consistency. Therefore, it seems that increasing concentration of lipid particle preserved the colloidal particle size similar to low-lipid concentration. However, Dynasan 118 and Compritol 888 ATO demonstrated larger particle size in higher lipid dispersion formulations. As described earlier

Table 3. Critical stress (σ_c), equilibrium storage modulus (G'_e), characteristic network relaxation time[a] (τ), and appearance of SLN dispersions at 20% (w/w) lipid.

Lipid at 20% (w/w) dispersion	σ_c (Pa)	G′e(Pa)	τ (seconds)	Appearance
Cetyl palmitate	0.5	20	0.63	Liquid
Dynasan 114	0.08	15	0.25	Liquid
Dynasan 116	N/A	N/A	N/A	Solid
Dynasan 118	N/A	N/A	N/A	Solid
Compritol 888 ATO	N/A	100,000	16	Soft wax

[a] $\tau = 1/(2\pi f_c)$, where f_c is a frequency at which tan δ is equal to 1.

Table 4. Mean particle diameter, polydispersity index (PDI), and zeta potential of SLN dispersions at 20% (w/w) lipid.

Lipid system	Hydrodynamic diameter (nm)	PDI	Zeta potential (mV)
Cetyl palmitate	165 ± 1	0.17 ± 0.01	−41.4 ± 1.1
Dynasan 114	199 ± 4	0.16 ± 0.01	−48.7 ± 0.5
Dynasan 116	183 ± 6	0.26 ± 0.04	−40.3 ± 0.6
Dynasan 118	395 ± 36	0.70 ± 0.02	−48.3 ± 1.5
Compritol 888 ATO	624 ± 41	0.67 ± 0.08	−38.5 ± 0.5

that PCS calculates particle size by assuming spherical shape, the determined values do not represent a correct dimension of nonspherical particles such as triglycerides. Therefore, the differences in the measured viscoelastic properties of lipid dispersions cannot be explained by data from particle size analysis.

Conclusion

This study characterized viscoelastic behaviors of SLN dispersions prepared from different types and concentrations of lipid. Various dispersion consistencies were observed ranging from liquid to solid. The dispersions were electrostatically stabilized by negative charges on particle surface with high absolute values of zeta potential. Particle size determination using PCS failed to explain the variation in dispersion consistency because of nonspherical shape of pure triglycerides and wax used in the prepared SLNs. Viscoelastic measurement by the nondestructive oscillatory experiment at low stress was therefore employed to reveal the internal microstructure developed within the dispersions. In addition, the comparison between types and concentrations of lipid and the obtained consistency was investigated. At 5% (w/w) lipid, among the pure triglycerides (>90% by weight of triglyceride), a more elastic consistency was found in the sequence of Dynasan 114 < Dynasan 116 < Dynasan 118 dispersions because of the formation of larger anisometric triglyceride nanocrystals of longer alkyl chains of fatty acid residues. Compritol 888 ATO particles

formed a less-ordered crystalline structure because of containing a mixture of mono-, di-, and triglycerides of mainly C22-fatty acid chains, thus, yielding the dispersion with less elastic property than Dynasan 118 and Dynasan 116 dispersions. With respect to the similar C16 fatty acid chain length, a dispersion of cetyl palmitate displayed the lower network strength than Dynasan 116 dispersion because of the lower ability of the wax to form a particle with dense crystal packing. By increasing lipid concentration, the dispersion consistency was enhanced as revealed by the increase in the magnitude of storage modulus and the network relaxation time. The enhanced network strength of SLN dispersions at high volume fraction of lipid was from the increased interaction between particles. The obtained results can be used to predict the performance of SLN matrix in the delivery systems.

Acknowledgments

The authors acknowledge the financial support from the Research, Development and Engineering (RD&E) Fund through National Nanotechnology Center (NANOTEC), National Science and Technology Development Agency (NSTDA), Thailand (Project No. NN-B-21-EN2-93-50-04). The authors also thank Dr. Asira Fuongfuchat for providing valuable suggestions.

Declaration of interest

The authors report no conflicts of interest. The authors alone are responsible for the content and writing of this paper.

References

1. Alonso MJ. (2004). Nanomedicines for overcoming biological barriers. Biomed Pharmacother, 58:168–72.
2. Nishiyama N, Kataoka K. (2006). Current state, achievements, and future prospects of polymeric micelles as nanocarriers for drug and gene delivery. Pharmacol Ther, 112:630–48.
3. Müller RH, Lucks JS. (1996). Medication vehicles made of solid lipid particles (solid lipid nanospheres-SLN). European patent 0605497.
4. Wissing SA, Müller RH. (2002). Solid lipid nanoparticles as carrier for sunscreens: In vitro release and in vivo skin penetration. J Control Release, 81:225–33.
5. Lim SJ, Lee MK, Kim CK. (2004). Altered chemical and biological activities of all-*trans* retinoic acid incorporated in solid lipid nanoparticle powders. J Control Release, 100:53–61.
6. Cavalli R, Gasco MR, Chetoni P, Burgalassi S, Saettone MF. (2002). Solid lipid nanoparticles (SLN) as ocular delivery system for tobramycin. Int J Pharm, 238:241–5.
7. Zhang N, Ping Q, Huang G, Xu W, Cheng Y, Han X. (2006). Lectin-modified solid lipid nanoparticles as carriers for oral administration of insulin. Int J Pharm, 327:153–9.
8. Müller RH, Mäder K, Gohla S. (2000). Solid lipid nanoparticles (SLN) for controlled drug delivery—a review of the state of art. Eur J Pharm Biopharm, 50:161–77.
9. Mehnert W, Mäder K. (2001). Solid lipid nanoparticles: Production, characterization and applications. Adv Drug Deliv Rev, 47:165–96.
10. Müller RH, Radtke M, Wissing SA. (2002). Solid lipid nanoparticles (SLN) and nanostructured lipid carriers (NLC) in cosmetic and dermatological preparations. Adv Drug Deliv Rev, 54:S131–55.
11. Hatziantoniou S, Deli G, Nikas Y, Demetzos C, Papaioannou GTh. (2007). Scanning electron microscopy study on nanoemulsions and solid lipid nanoparticles containing high amounts of ceramides. Micron, 38:819–23.
12. Illing A, Unruh T. (2004). Investigation on the flow behavior of dispersions of solid triglyceride nanoparticles. Int J Pharm, 284:123–31.
13. Michailova V, Titeva St, Kotsikova R, Krusteva E, Minkov E. (1999). Influence of aqueous medium on viscoelastic properties of carboxymethylcellulose sodium, hydroxypropylmethyl cellulose, and thermally pre-gelatinized starch gels. Colloids Surf A Physicochem Eng Asp, 149:515–20.
14. Kavanagh GM, Ross-Murphy SB. (1998). Rheological characterization of polymer gels. Prog Polym Sci, 23:533–62.
15. Gunasekaran S, Ak Mehmet M. (2000). Dynamic oscillatory shear testing of foods-selected applications. Trends Food Sci Technol, 11:115–27.
16. Brummer R. (2006). Rheology essentials of cosmetic and food emulsions. Hamburg, Germany: Springer.
17. Bunjes H, Westesen K, Koch MHJ. (1996). Crystallization tendency and polymorphic transitions in triglyceride nanoparticles. Int J Pharm, 129:159–73.
18. Jenning V, Schäfer-Korting M, Gohla S. (2000). Vitamin A-loaded solid lipid nanoparticles for topical use: Drug release properties. J Control Release, 66:115–26.
19. Souto SB, Anselmi C, Centini M, Müller RH. (2005). Preparation and characterization of n-dodecyl-ferulate-loaded solid lipid nanoparticles (SLN). Int J Pharm, 295(1–2):261–8.
20. Ruktanonchai U, Limpakdee S, Meejoo S, Sakulkhu U, Bunyapraphatsara N, Junyaprasert V, et al. (2008). The effect of cetyl palmitate crystallinity on physical properties of gamma-oryzanol encapsulated in solid lipid nanoparticles. Nanotechnology, 19:1–10.
21. Lippacher A, Müller RH, Mäder K. (2002). Semisolid SLN dispersions for topical application: Influence of formulation and production parameters on microstructure. Eur J Pharm Biopharm, 53:155–60.
22. Souto EB, Wissing SA, Barbosa CM, Müller RH. (2004). Comparative study between the viscoelastic behaviors of different lipid nanoparticle formulations. J Cosmet Sci, 55:463–71.
23. Lippacher A, Müller RH, Mäder K. (2004). Liquid and semisolid SLN™ dispersions for topical application: Rheological characterization. Eur J Pharm Biopharm, 58:561–7.
24. Junyaprasert VB, Teeranachaideekul V, Souto EB, Boonme P, Müller RH. (2009). Q_{10}-loaded NLC versus nanoemulsions: Stability, rheology and *in vitro* skin permeation. Int J Pharm, 377:207–14.
25. Seetapan N, Bejrapha P, Srinuanchai W, Ruktanonchai UR. (2010). Rheological and morphological characterizations on physical stability of gamma-oryzanol-loaded solid lipid nanoparticles (SLNs). Micron, 41:51–8.
26. Radomska-Soukharev A. (2007). Stability of lipid excipients in solid lipid nanoparticles. Adv Drug Deliv Rev, 59:411–8.
27. Tadros TF. (1996). Correlation of viscoelastic properties of stable and flocculated suspensions with their interparticle interactions. Adv Colloid Interface Sci, 68:97–200.
28. Ferry JD. (1980). Viscoelastic properties of polymers. New York, USA: John Wiley Sons Inc.
29. Macosko CW. (1994). Rheology principles, measurements, and applications. New York, USA: VCH Publishers.
30. Souto EB, Müller RH. (2005). SLN and NLC for topical delivery of ketoconazole. J Microencapsul, 22:501–10.
31. Westesen K, Siekmann B. (1997). Investigation on the gel formation of phospholipid-stabilized solid lipid nanoparticles. Int J Pharm, 151:35–45.

32. Siekmann B, Westesen K. (1998). Submicron lipid suspensions (solid lipid nanoparticles) versus lipid nanoemulsions: Similarities and differences. In: Benita S, ed. Submicron emulsions in drug targeting and delivery. Amsterdam: Harwood, 205–18.
33. Benna M, Kbir-Ariguib N, Clinard C, Bergaya F. (2002). Cardhouse microstructure of purified sodium montmorillonite gels evidenced by filtration properties at different pH. Prog Colloid Polym Sci, 117:204–10.
34. Sein A, Verheij JA, Agterof WGM. (2002). Rheological characterization, crystallization, and gelation behavior of monoglyceride gels. J Colloid Interface Sci, 249:412–22.
35. Clarke B. (1967). Rheology of coarse settling suspensions. Trans Inst Chem Eng, 45:251–6.
36. Brown JP, Pinder KL. (1971). Time dependent rheology of artificial slurries. Can J Chem Eng, 49:38–43.
37. Freitas C, Müller RH. (1998). Effect of light and temperature on zeta potential and physical stability in solid lipid nanoparticle (SLN™) dispersions. Int J Pharm, 168:221–9.
38. zur Mühlen A. (1996). Feste lipid Nanopartikel mit Prolongierter Wirkstoffliberation. Herstellung, Langzeitstabilität Charakterisierung, Freisetzungsverhalten und -mechanismen. Ph.D. thesis, Freie Universität Berlin, Berlin, Germany.